Electronic Supplementary Material (ESI) for Journal of Materials Chemistry A.

Supporting Information

Mutually Beneficial Co_3O_4@MoS_2 Heterostructures as Highly Efficient Bifunctional Catalyst for Electrochemical Overall-Water-Splitting

Jia Liu[a,1], Jinsong Wang[a,1], Bao Zhang[a], Yunjun Ruan[a], Houzhao Wan[b], Xiao Ji[a], Kui Xu[a], Dace Zha[a], Ling Miao[a,*], Jianjun Jiang[a,*]

[a] School of Optical and Electronic Information, Huazhong University of Science and Technology, Wuhan 430074, PR China. *E-mail: miaoling@mail.hust.edu.cn; jiangjj@mail.hust.edu.cn

[b] Hubei Collaborative Innovation Center for Advanced Organic Chemical Materials, Faculty of Physics and Electronic Science, Hubei University, Wuhan 430062, China

[1] These authors contributed equally to this work

1. Computational methods

DFT calculations were performed using the Vienna Ab Initio Simulation Package (VASP),[1, 2] and the projector augmented wave method (PAW)[3] is adopted for the treatment of core electrons, the exchange-correlation function is described by the Perdew, Burke, and Ernzerhof (PBE) version of the generalized gradient approximation (GGA) plus Hubbard-Uframework.[4, 5] The value of U = 3.52 eV was used for the Coulomb corrections to the Co 3d states. The energy cut-off for the plane-wave basis was set to 460eV for all calculations. Conjugated gradient method was used to the geometry optimization and all the atomic coordinates were fully relaxed until the maximal force on each atom was less than 0.05 eV/Å, and the convergence condition for energy is 10^{-4} eV. All constructions possess larger than 15 Å vacuum region in the z direction to minimize the interactions between adjacent image cells.

1.1 HER calculation

The free energy was calculated using the equation:[6]

$$G = E + ZPE - TS$$

where *G, E, ZPE* and *TS* are the free energy, total energy from DFT calculations, zero point energy and entropic contributions (T was set to be 300K), respectively. *ZPE* and *TS* could be are retrieved from literature.[7]

1.2 OER calculation

The thermodynamic model of water oxidation proposed by Norskov and co-workers,[7] which is composed of four electrochemical steps, each of which constitutes one proton transfer, were used in this work. The following electron reaction paths are considered for oxygen evolution reaction (OER) process:

$$H_2O(l) + * \rightleftharpoons HO* + H^+ + e^- \ (\Delta G_1) \tag{1}$$

$$HO* \rightleftharpoons O* + H^+ + e^- \ (\Delta G_2) \tag{2}$$

$$O* + H_2O(l) \rightleftharpoons HOO* + H^+ + e^- \ (\Delta G_3) \tag{3}$$

$$HOO* \rightleftharpoons O_2(g) + * + H^+ + e^- \ (\Delta G_4) \tag{4}$$

where * represents an active site on the surface, ΔG_{1-4} are the free energies of adsorption for the above four elementary steps,

The free energies of adsorption are calculated as follows:

$$\Delta G_1 = E_{DFT}^{HO*} - E_{DFT}^{*} + \frac{1}{2} E_{DFT}^{H2(g)} - E_{DFT}^{H2O(l)} + \Delta ZPE - T\Delta S$$

$$\Delta G_2 = E_{DFT}^{O*} - E_{DFT}^{HO*} + \frac{1}{2} E_{DFT}^{H2(g)} + \Delta ZPE - T\Delta S$$

$$\Delta G_3 = E_{DFT}^{HOO*} - E_{DFT}^{O*} + \frac{1}{2} E_{DFT}^{H2(g)} - E_{DFT}^{H2O(l)} + \Delta ZPE - T\Delta S$$

$$\Delta G_4 = E_{DFT}^{*} - E_{DFT}^{HOO*} + 2E_{DFT}^{H2O(l)} - \frac{3}{2} E_{DFT}^{H2(g)} + 4.92 + \Delta ZPE - T\Delta S$$

where E_{DFT} is energy from density functional theory calculation. The ZPE and entropy at 298 K (S) are retrieved from literature.[8]

The catalytic activity of the above process is controlled by the potential limiting step (PLS) which has the maximum free energies of adsorption (ΔG_{1-4}^{0}). Thus, the theoretical overpotential η is evaluated by the following equation:

$$\eta = max[\Delta G_1, \Delta G_2, \Delta G_3, \Delta G_4]/e - 1.23\ [V]$$

2. Experimental section

2.1. Materials synthesis

The Co_3O_4@MoS_2 heterostructures on carbon cloth were synthesized by a simple two-step hydrothermal reaction. Firstly, to fabricate the MoS_2 nanosheet arrays, 2 mmol sodium molybdate ($Na_2MoO_4 \cdot 2H_2O$) and 8 mmol thiourea (CH_4N_2S) were mixed together in 60 ml deionized (DI) water, then stirring for 15 min to obtained a clear solution. The solution was transferred into Teflon-lined stainless-cleaned 100 ml autoclave. Before using the carbon cloth as a substrate to *in situ* grown the arrays, it was washed with DI water and ethanol to clean the surface. Then, the surface-cleaned carbon cloth (2 cm × 4 cm) was immersed into the solution. The hydrothermal reaction was conducted at 200 ℃ for 24 h. The as-obtained MoS_2 nanosheet arrays were rinsed with DI water and ethanol at least three times and then dried naturally at room temperature. Secondly, 0.6 mmol cobalt acetate tetrahydrate was added into 52 ml DI water with stirring for 10 min to obtain a pink solution. Subsequently, 8 mL NH_4OH (25%) were added to the solution, the above carbon cloth was immersed into the solution. Then the solution was transferred into Teflon-lined stainless-cleaned 100 ml autoclave and maintained at 180 ℃ for 3 h. After cooling to room temperature, the carbon cloth was wash several times with DI water and ethanol, respectively, followed by drying at 60 ℃。

2.2. Characterization

The phase formation was identified using powder XRD (Philips X'pert PRO; Cu Kα, λ= 0.1524 nm). The morphologies of the catalysts were observed by scanning electron microscope (SEM FEI Quanta 200, FESEM JEOL JSM-7100F) and transmission electron microscopy (TEM F20). The X-ray photoelectron spectroscopy (XPS) spectra were measured on Kratos AXIS Ultra DLD-600W XPS system equipped with a monochromatic Al Kα (1486.6 eV) as X-ray source.

2.3. Electrochemical Measurements

All electrochemical tests were carried out by using CHI760e electrochemical workstation. The Ag/AgCl (saturated KCl solution) was used as the reference electrode, platinum foil was served as the counter electrode, and the synthesized Co_3O_4@MoS_2**/**CC was utilized as working electrode. All electrochemical tests were performed in 1 M KOH aqueous electrolyte. For the HER performance, LSV were measured from -0.9 to -1.4 V versus saturated Ag/AgCl at a scan rate of 5 mV s^{-1}. And the OER performance, all linear sweep voltammograms (LSV) were measured from 0 to 0.7 V at a scan rate of 2 mV s^{-1}. Chronoamperometric measurements were performed at corresponding potential to deliver a current density of 10 mA cm^{-2}. The overpotentials were obtained from the intersection of the tangents of LSV current and the polarization curve baseline. The potential converted to RHE scale by using the equation $E_{RHE}=E_{Ag/AgCl} + 0.197 + 0.059 \times pH$, where E_{RHE} is the potential referred to RHE and $E_{Ag/AgCl}$ is the measured potential against Ag/AgCl reference electrode. The electrochemically active surface areas (ECSAs) can be observed from the electrochemical double layer capacitance (C_{dl}) through collecting cyclic voltammograms (CVs), CV tests with different scan rates (1, 2, 3, 4, 5 and 6 mV·s^{-1}) in the potential range from 0.1 to 0.2 V versus RHE. The electrochemical impedance spectroscopy (EIS) measurements were carried out by ranging the frequency from 100 kHz to 0.1 Hz.

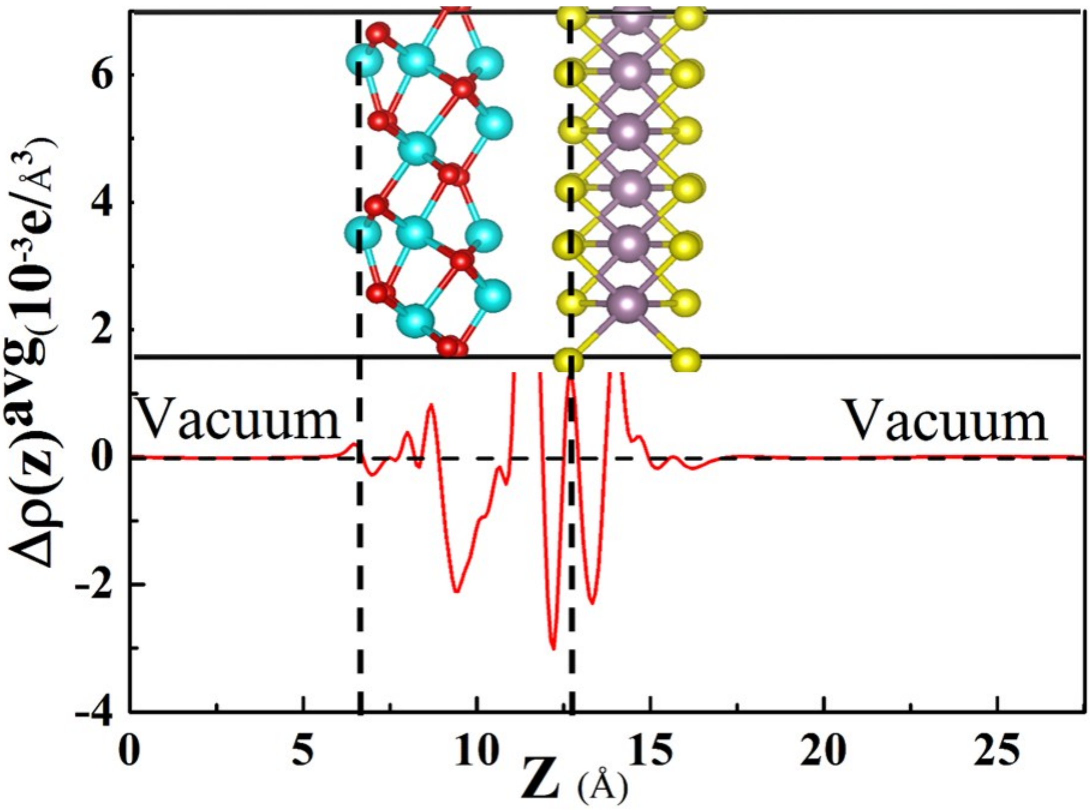

Fig. S1 isosurface of local charge density difference of Co_3O_4@MoS_2 interface.

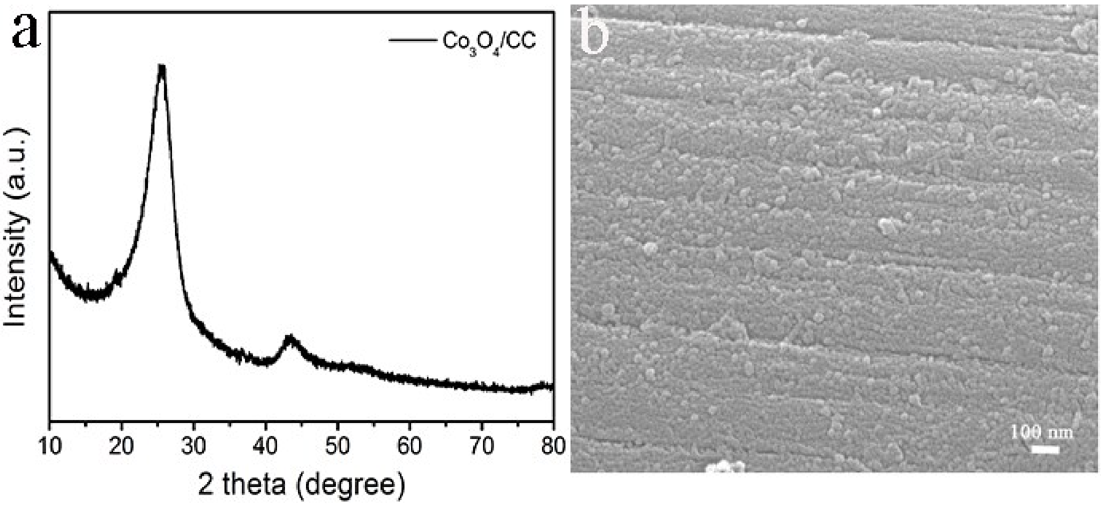

Fig. S2 (a) The XRD pattern of Co_3O_4/CC; (b) the SEM images of Co_3O_4/CC.

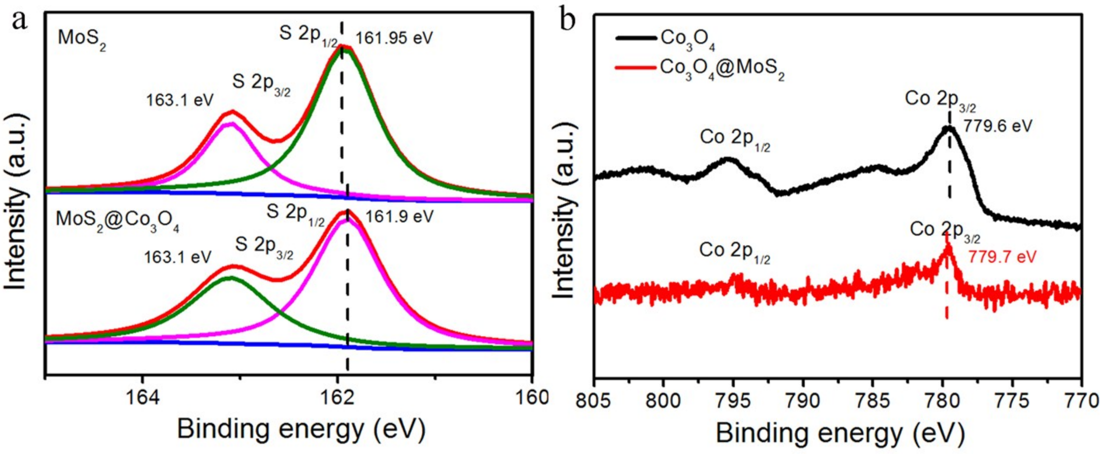

Fig. S3 (a) the S XPS spectra of MoS$_2$/CC and Co$_3$O$_4$@MoS$_2$/CC; (b) the Co XPS spectra of Co$_3$O$_4$/CC and Co$_3$O$_4$@MoS$_2$/CC.

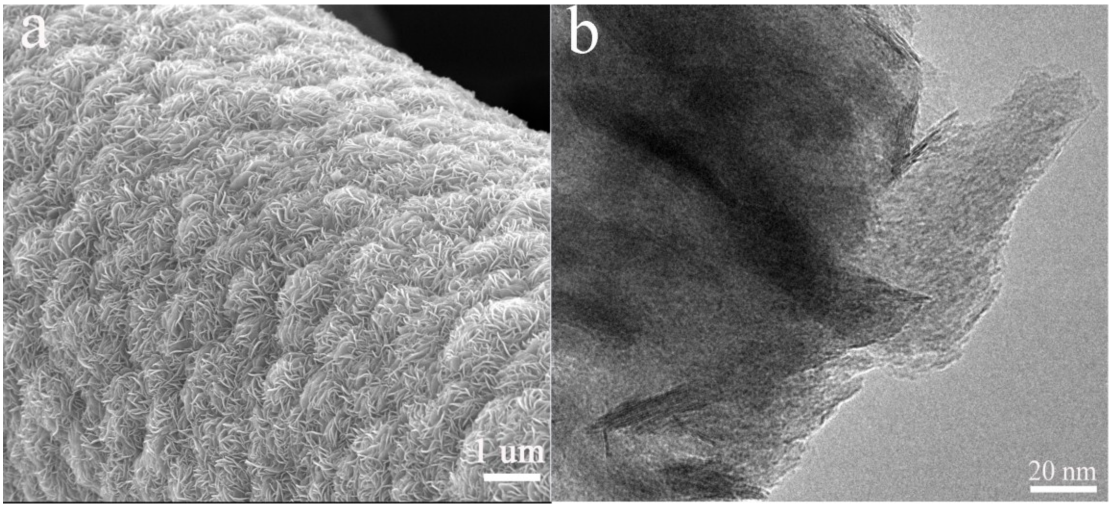

Fig. S4 (a) The SEM image of MoS_2; (b) TEM image of MoS_2.

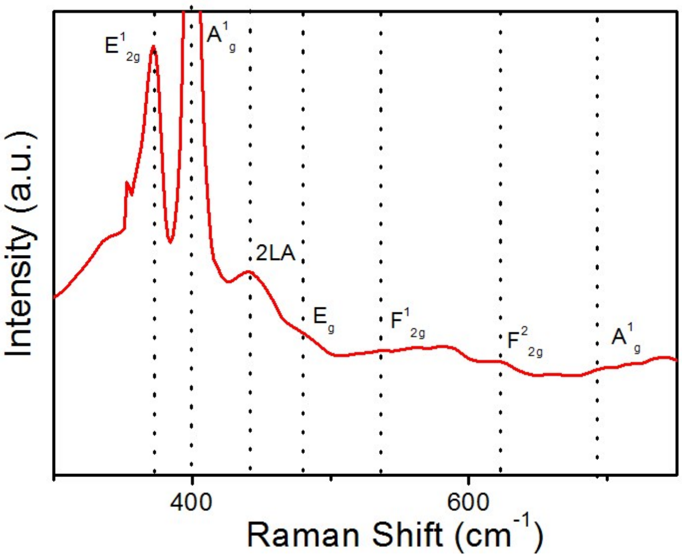

Fig. S5 the Raman spectra of Co_3O_4@MoS_2/CC.

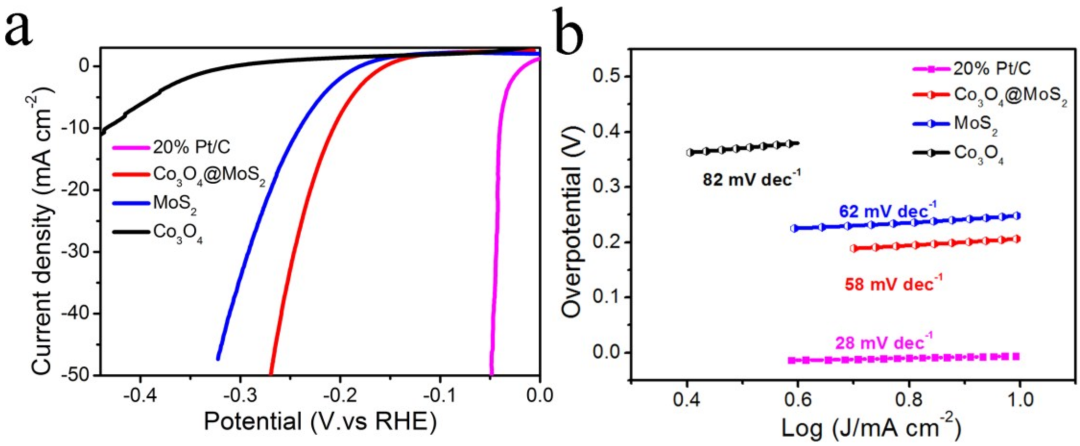

Fig. S6 Electrochemical characterization of hydrogen evolution reaction. (a) Polarizaiton curves (b) corresponding Tafel plots of 20% Pt/C, MoS_2, Co_3O_4 and Co_3O_4@MoS_2 in 1 M KOH. Scan rate: 5 mV s^{-1}.

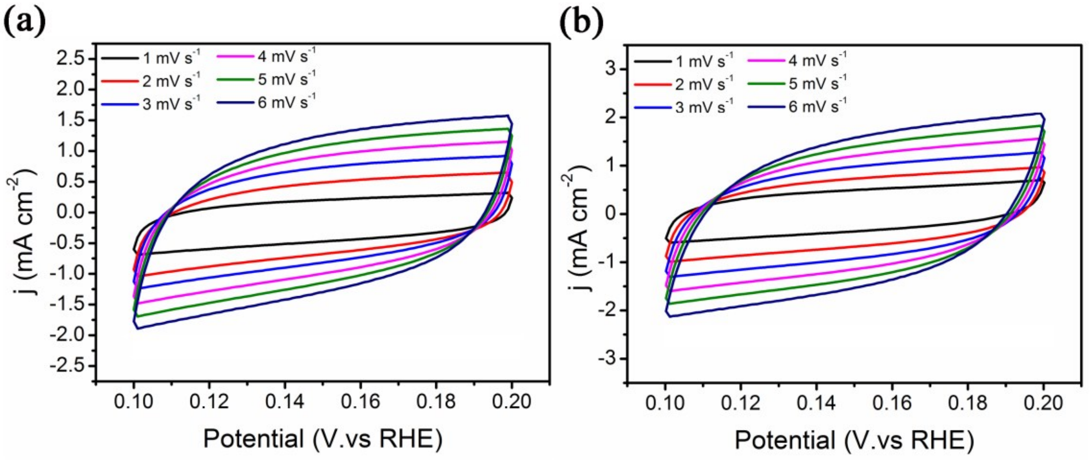

Fig. S7 Cyclic voltammograms at different scan rates in the region between -100 and -200 mV (vs. RHE): (a) Co_3O_4@MoS_2, (b) MoS_2

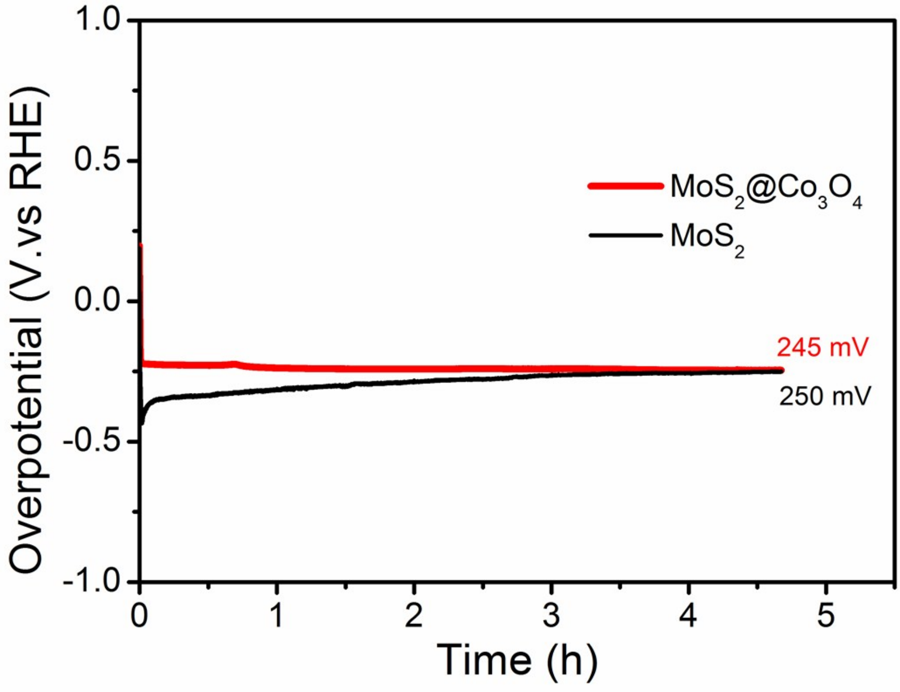

Fig. S8 the stability of Co_3O_4/CC and Co_3O_4@MoS_2/CC in acid solution.

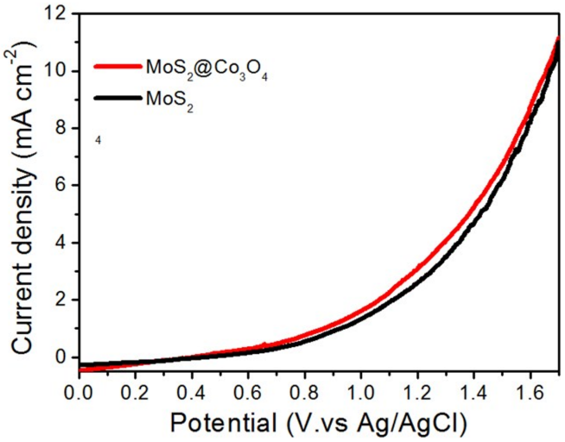

Fig. S9. The OER polarizaiton curves of MoS_2, Co_3O_4 and Co_3O_4@MoS_2 in 0.5 M H_2SO_4. Scan rate: 2 mV s^{-1}.

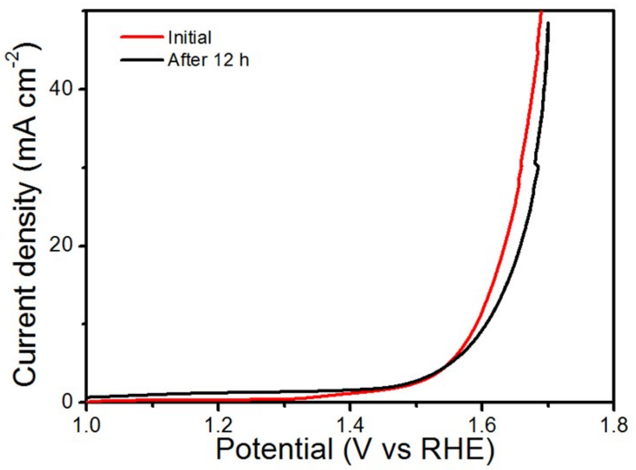

Fig. S10 the LSV of water splitting after long time test.

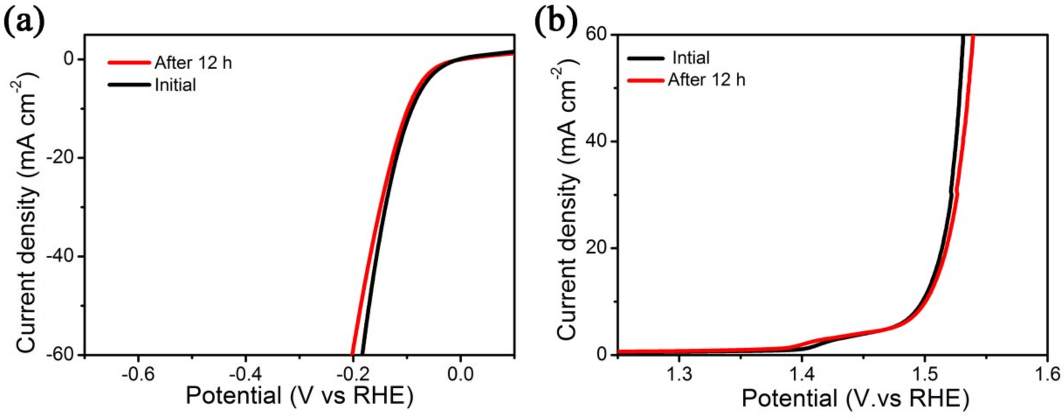

Fig. S11 (a, b) The stability of Co_3O_4@MoS_2/CC for HER and OER.

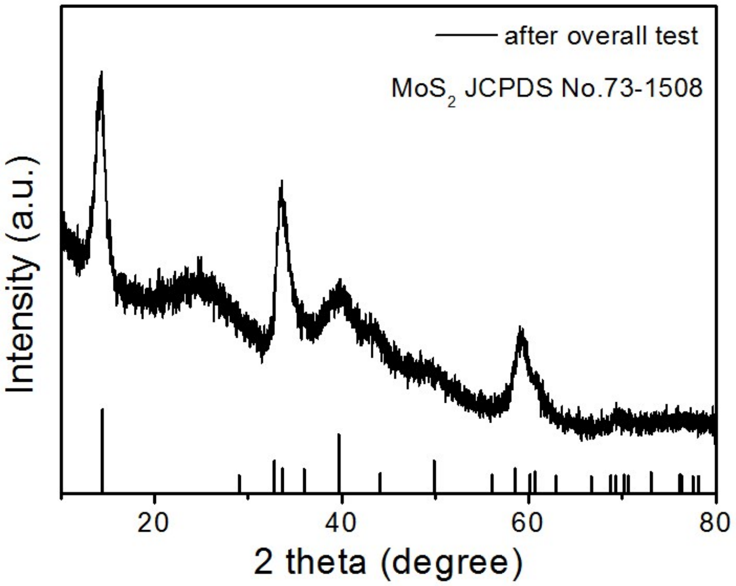

Fig. S12 The XRD patterns after overall test.

Table S1. Comparison of two electrode water splitting voltage of Co_3O_4@MoS_2/CC electrocatalysts with other bifunctional electrocatalysts.

Catalyst	Electrolyte	Overall voltage (V)@10 mA cm^{-2}	Ref.
Co_3O_4@MoS_2/CC	1 M KOH	1.59 V	This work
$NiCo_2S_4$/NF	1 M KOH	1.63 V	[9]
NiFe/$NiCo_2O_4$/NF	1 M KOH	1.67 V	[10]
MoS_2/Ni_3S_2/NF	1 M KOH	1.56 V	[11]
CoS-Co(OH)$_2$@aMoS_{2+x}/NF	1 M KOH	1.58 V	[12]
RuO_2/Co_3O_4	1 M KOH	1.645 V	[13]

Reference

1. G. Kresse and J. Hafner, *Phys. Rev. B*, 1994, **49**, 14251.
2. G. Kresse and J. Furthmüller, *Phys. Rev. B*, 1996, **54**, 11169.
3. P. E. Blöchl, *Phys. Rev. B*, 1994, **50**, 17953.
4. J. P. Perdew, K. Burke and M. Ernzerhof, *Phys. Rev. Lett.*, 1996, **77**, 3865.
5. W. Kohn and L. J. Sham, *Physical review*, 1965, **140**, A1133.
6. J. K. Norskov, T. Bligaard, A. Logadottir, J. R. Kitchin, J. G. Chen, S. Pandelov and U. Stimming, *PLoS One*, 2005, **5**, e12154-e12154.
7. I. C. Man, H. Y. Su, F. Calle-Vallejo, H. A. Hansen, J. I. Martínez, N. G. Inoglu, J. Kitchin, T. F. Jaramillo, J. K. Nørskov and J. Rossmeisl, *ChemCatChem*, 2011, **3**, 1159-1165.
8. H. H. Pham, M.-J. Cheng, H. Frei and L.-W. Wang, *ACS Catal*, 2016, **6**, 5610-5617.
9. A. Sivanantham, P. Ganesan and S. Shanmugam, *Adv. Funct. Mater*, 2016, **26**, 4661-4672.
10. C. Xiao, Y. Li, X. Lu and C. Zhao, *Adv. Funct. Mater*, 2016, **26**, 3515-3523.
11. J. Zhang, T. Wang, D. Pohl, B. Rellinghaus, R. Dong, S. Liu, X. Zhuang and X. Feng, *Angew. Chem. Int. Ed*, 2016, **128**, 6814-6819.
12. T. Yoon and K. S. Kim, *Adv. Funct. Mater*, 2016, **26**, 7386-7393.
13. H. Liu, G. Xia, R. Zhang, P. Jiang, J. Chen and Q. Chen, *RSC Adv*, 2017, **7**, 3686-3694.